MULTI-FUNCTIONAL MBIT FOR PEPTIDE TANDEM MASS SPECTROMETRY

Hye-Joo Yoon, Jongcheol Seo, and Seung Koo Shin*

Bio-Nanotechnology Center, Department of Chemistry, Pohang University of Science and Technology, Pohang, Korea

Received 8 November 2012; revised 20 November 2013; accepted 26 March 2014

Published online 28 May 2014 in Wiley Online Library (wileyonlinelibrary.com). DOI 10.1002/mas.21435

Isobaric tags have been widely used for the identification and quantification of proteins in mass spectrometry-based proteomics. The mass-balanced, $^{1}H/^{2}H$ isotope-coded dipeptide tag (MBIT) is a multifunctional isobaric tag based on N-acetyl-Ala-Ala dipeptide containing an amine-reactive linker that conjugates the tag to the primary amines of proteolytic peptides. MBITs provide a pair of isotope-coded quantitation signals separated by 3 Da, which enables 2-plex quantification and identification of proteins in the 15–250 fmol range. Various MBITs diversified at the N-acetyl group or at the side chain of the first alanine provide a pair of $\boldsymbol{b}$*s ions as low-mass quantitation signals in a distinct mass window. Thus, a combination of different MBITs allows multiplex quantification of proteins in a single liquid chromatography-mass spectrometry experiment. Unlike other isobaric tags, MBITs also offer a pair of* $\boldsymbol{y}$*s ions as high-mass quantitation signals in a noise-free region, facilitating protein quantification in quadrupole ion trap mass spectrometers. Uniquely,* $\boldsymbol{b}_S$ *ions, forming N-protonated oxazolone, undergo unimolecular dissociation and generate the secondary low-mass quantitation signals,* $\boldsymbol{a}_S$ *ions. The yield of* $\boldsymbol{a}_S$ *ions derived from* $\boldsymbol{b}_S$ *ions can be used to measure the temperature of* $\boldsymbol{b}_S$ *ions, which enables a reproducible acquisition of the peptide tandem mass spectra. Thus, MBITs enable multiplexed quantitation of proteins and the concurrent measurement of ion temperature using* $\boldsymbol{b}_S$ *and* $\boldsymbol{a}_S$ *signal ions as well as the isobaric protein quantitation in resonance-type ion trap using* $\boldsymbol{y}_S$ *(complement of* $\boldsymbol{b}_S$*) signal ions. This review provides an overview of MBITs with a focus on the multi-functionality that has been successfully demonstrated in the peptide tandem mass spectrometry.* © 2014 The Authors. *Mass Spectrometry Reviews* published by Wiley Periodicals, Inc. Mass Spec Rev 34:209–218, 2015

Keywords: *MBIT; isobaric tag; tandem mass spectrometry; multiplexed protein quantitation; ion temperature measurement*

I. INTRODUCTION

The tandem mass spectra of peptides provide sequence information that allows the identification of proteins from the proteome database (Biemann & Martin, 1987; Eng, McCormack, & Yates, 1994; Dongré et al., 1996; Aebersold & Mann, 2003). However, the peptide fragment spectra alone present no quantitative information about identified proteins (Gygi et al., 1999). Isobaric tags are designed to enable the quantification of proteins simultaneously with the identification using tandem mass spectrometry (MS/MS) (Thompson et al., 2003; Ong & Mann, 2005). They consist of two or more molecules of the same mass, but each molecule is differentially encoded with stable isotopes for multiplexed protein quantification. The MS/MS analysis of the tagged peptide ions presents distinct isotope-coded fragment ions derived from isobaric tags as quantitation signals. The intensity ratio of quantitation signals provides information about the relative amount of peptides or proteins initially labeled with the tags. Because those tagged peptides co-elute at the same time in liquid chromatography (LC), the quantitative proteome analysis can be carried out at high throughput by using LC-MS/MS (Rodríguez-Suárez & Whetton, 2013).

Several isobaric tags are available to date, which include isobaric tags for relative and absolute quantitation (iTRAQ) (Ross et al., 2004; Choe et al., 2007), the tandem mass tag (TMT) (Dayon et al., 2008, 2010), the cysteine-specific cleavable isobaric labeled affinity tag (CILAT) (Li & Zeng, 2007; Zeng & Li, 2009a), the deuterium isobaric amine-reactive tag (DiART) (Zeng & Li, 2009b; Zhang, Wang, & Li, 2010), the N,N-dimethylated leucine tag (DiLeu) (Xiang et al., 2010), and the Caltech isobaric tag (CIT) (Sohn et al., 2012).

They employ N,N-alkylated tertiary amines, which are encoded with $^{1}H/^{2}H$, $^{12}C/^{13}C$, $^{14}N/^{15}N$, and $^{16}O/^{18}O$ isotopes, to yield strong iminium or diazenium ions as quantitation signals. For instance, iTRAQ incorporates carbon, nitrogen, and oxygen isotopes in the *N*-methylpiperazine acetic acid ester group. TMT adopts carbon and nitrogen isotopes in the dimethylpiperidine moiety. CILAT contains hydrogen, carbon, and nitrogen isotopes in the piperazine derivative. DiART employs hydrogen, carbon, and nitrogen isotopes in the *N,N*-dimethylleucine moiety, whereas DiLeu utilizes hydrogen, carbon, nitrogen, and oxygen isotopes in N,N-dimethylated leucine. CIT uses hydrogen isotopes in the N,N-alkylated alanine residue.

The 4-plex iTRAQ reports quantitation signals at *m/z* 114–117 (Ross et al., 2004) and the 8-plex version provides signals at *m/z* 113–119 and 121 (Choe et al., 2007). TMT shows 6-plex signals at *m/z* 126–131 (Dayon et al., 2008) and can be extended to 8-plex tags (McAlister et al., 2012). CILAT exhibits up to 12-plex signals at *m/z* 130–142 (Zeng & Li, 2009a). DiART

The copyright line for this article was changed on 17 November 2015 after original online publication.

This is an open access article under the terms of the Creative Commons Attribution-NonCommercial-NoDerivs License, which permits use and distribution in any medium, provided the original work is properly cited, the use is non-commercial and no modifications or adaptations are made.

Contract grant sponsor: Functional Proteomics Center; Contract grant number: FPR08A1-040; Contract grant sponsor: National Research Foundation; Contract grant number: 2009-0086218.

Correspondence to: Seung Koo Shin, Department of Chemistry, Pohang University of Science and Technology, San 31 Hyoja-dong Nam-gu, Pohang, Korea 790-784. E-mail: skshin@postech.ac.kr

© 2014 The Authors. *Mass Spectrometry Reviews* published by Wiley Periodicals, Inc.

yields 6-plex signals at *m/z* 114–119, whereas DiLeu presents 4-plex signals at *m/z* 115–118. CIT reports signals at *m/z* 164 and 169.

Although these isobaric tags have been widely used in MS-based quantitative proteomics, their applications are somewhat constrained by the reagent cost and the multiplexing capability is often compromised by overlapping small peptide fragments in the quantitation signal region. Overlaps in precursor peptides also reduce the quantitation accuracy, because the concurrent selection of multiple species frequently occurs in the 1–3 Da MS/MS isolation window (Wenger et al., 2011). In addition, the interference of adjacent quantitation signals with their natural isotope peaks is a downside of 1-Da gap multiplexed signals. Moreover, these isobaric tags reporting low-mass signals are not applicable to ion trap mass spectrometers, one of the most popular platforms for MS-based proteomics, because of the low mass cutoff inherent in the resonance type ion trap.

We have developed an alternative isobaric tag referred to "mass-balanced $^{1}H/^{2}H$-isotope dipeptide tag" (MBIT) (Seo et al., 2008) to overcome some of these difficulties. MBITs can be readily synthesized at low cost in the laboratory (Seo et al., 2008; Suh et al., 2011). They offer a pair of 3-Da gap quantitation signals in both low- and high-mass regions with no or little overlapping peptide fragments. Thus, MBITs can be employed in ion trap for the isobaric protein quantification (Seo, Yoon, & Shin, 2011). The signal mass window of MBITs can be varied by diversifying the dipeptide structure (Seo et al., 2008; Suh et al., 2011). The signal-variable MBITs can be combined together for multiplexed protein quantification (Suh et al., 2011). MBITs can also be used as internal temperature standards for the ion temperature measurement (Seo et al., 2012). This review focuses on these multi-functionalities of MBITs which have been demonstrated with a number of model peptides and proteins as well as yeast heat shock proteins.

II. CONCEPT AND FUNTIONALITY OF MBIT

MBITs are based on the *N*-acetyl-Xaa-Ala dipeptide (Fig. 1). The $^{1}H/^{2}H$ isotopes are differentially encoded at the methyl groups of the *N*-acetyl moiety and alanine as CH_3/CD_3 or CD_3/CH_3. Resulting $^{1}H/^{2}H$-isotope-coded dipeptides are isobaric. The *C*-termini of the dipeptides are derivatized either to *N*-succinimidyl ester (OSu) or to benzotriazol-1-yl ester which is amine-reactive. These isobaric, amine-reactive chemical modifications yield 2-plex MBITs (CH_3/CD_3-and CD_3/CH_3-forms) (Seo et al., 2008).

MBITs can be linked to the *N*-terminal primary amine and the lysinyl ε-amine of proteolytic peptides to produce *N*-acetyl-Xaa-Ala-peptides. The 2-plex MBIT-linked peptides appear at the same position in the mass spectra as isotopomers. Upon collision-induced dissociation (CID) of the isobaric *N*-acetyl-Xaa-Ala-peptides, amide-bond cleavage (Nold et al., 1997; Paizs & Suhai, 2005) between Xaa and Ala results in both the b-type signal ion ($\mathbf{b}_S$) and the y-type signal ion ($\mathbf{y}_S$), which are complementary to each other (for the nomenclature, see the reference, Roepstorff & Fohlman, 1984). The $\mathbf{b}_S$ ions, which are low-mass quantitation signals, consist of the isotope-coded *N*-acetyl-Xaa moiety that forms the structure of N-protonated oxazolone (Paizs et al., 1999; Polfer et al., 2005; Yoon et al.,

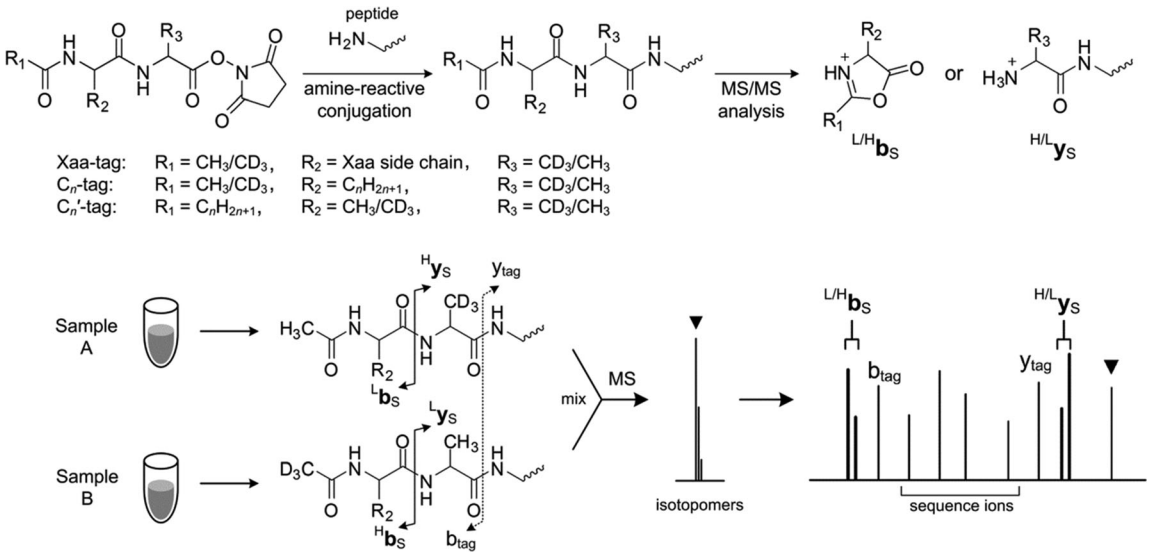

FIGURE 1. Schematic of peptide quantitation using MBIT. MBIT is conjugated to the *N*-terminus of peptide via the *N*-succinimide ester (OSu) linker. The $^{1}H/^{2}H$-isotopes are encoded in R_1 and R_3 for the Xaa- and C_n-tags and in R_2 and R_3 for the C_n'-tag. The Xaa-tag contains the side chain of natural amino acids in place of R_2. The C_n-tag has a linear alkyl side chain (C_nH_{2n+1}) in place of R_2, whereas the C_n'-tag carries C_nH_{2n+1} in place of R_1. The C_1-tag is the same as the Ala-tag and an isomer of the C_1'-tag. Upon tandem mass analysis, MBIT-linked peptides produce both b-type low-mass quantitation signals ($^{L/H}\mathbf{b}_S$; N-protonated oxazolone ion) and y-type high-mass quantitation signals ($^{H/L}\mathbf{y}_S$; protonated Ala-peptide), which are complementary to each other. Of the 2-plex MBITs, the CH_3/CD_3-form is conjugated to proteolytic peptides in sample A, whereas the CD_3/CH_3-form is conjugated to those in sample B. The 2-plex MBIT-linked peptides are mixed together and analyzed by tandem mass spectrometry. The mass spectra show the MBIT-linked peptides at the same position as isotopomers and the tandem mass spectra of the mass-selected MBIT-linked peptides present $^{L/H}\mathbf{b}_S$ and $^{H/L}\mathbf{y}_S$ quantitation signals for 2-plex quantification of peptides as well as sequence ions for peptide idenfication.

2008). The $\mathbf{y}_S$ ions, which are high-mass quantitation signals, contain the isotope-coded alanine in the form of protonated Ala-peptide. Because of the $^1H/^2H$-isotope-coded methyl groups of the *N*-acetyl moiety and alanine, both $\mathbf{b}_S$ and $\mathbf{y}_S$ ions appear as doublets ($^{L/H}\mathbf{b}_S$ and $^{H/L}\mathbf{y}_S$; L: light, H: heavy) and each doublet is separated by 3 Da, which is the mass difference between CH_3 and CD_3. In most cases, this 3 Da gap is wide enough to avoid overlaps with natural isotope peaks of the doublet signal ions. The signal intensity ratio, $[^L\mathbf{b}_S]/[^H\mathbf{b}_S]$ or $[^H\mathbf{y}_S]/[^L\mathbf{y}_S]$, represents the abundance ratio of two identical peptides differentially labeled with 2-plex MBITs. On the other hand, amide-bond cleavage in other regions of the peptides generates amino acid sequence ions as singlets. Therefore, the singlet sequence ions allow the identification of proteins and the doublet signal ions afford the quantification of the identified proteins.

The amino acid Xaa in MBIT can be varied by changing its side chain, enabling the mass shift of the $\mathbf{b}_S$ doublet in the tandem mass spectra of 2-plex MBIT-linked peptides (Fig. 2). Of the natural amino acids, alanine, serine, valine, glutamine, histidine, phenylalanine, arginine, and tyrosine in place of Xaa yield the $\mathbf{b}_S$ doublet at *m/z* 114/117, 130/133, 142/145, 171/174, 180/183, 190/193, 199/202, and 206/209, respectively (Seo et al., 2008). These MBITs are called Ala-, Ser-, Val-, Gln-, His-, Phe-, Arg-, and Tyr-tags. Artificial amino acids (C_n: alanine with a linear alkyl side chain C_nH_{2n+1}, $n = 1$–8) in place of Xaa yield the $\mathbf{b}_S$ doublet at *m/z* 114/117, 128/131, 142/145, 156/159, 170/173, 184/187, 198/201, and 212/215, respectively (Suh et al., 2011). They are called the aliphatic C_n-tags. Note that the C_1-tag is the Ala-tag. The isomeric form of the aliphatic C_n-tag, *N*-acyl-Ala-Ala, is called the acyl C_n'-tag, where a linear alkyl chain is placed at the *N*-acyl group ($C_nH_{2n+1}CO$) and the $^1H/^2H$-isotopes are differentially encoded at the methyl groups of the first and second alanines (Seo et al., 2012). The acyl C_n'-tag ($n = 1$–8) presents the $\mathbf{b}_S$ doublet at the same position as the aliphatic C_n-tag; however, their $\mathbf{b}_S$ ions are structural isomers. In brief, while the mass window of the $\mathbf{b}_S$ doublet is set between *m/z* 100 and 220, which is comparable to other isobaric tags, MBITs are uniquely designed to vary the signal mass window and avoid interference from immonium, y-type, and other internal fragment ions (Seo et al., 2008). These

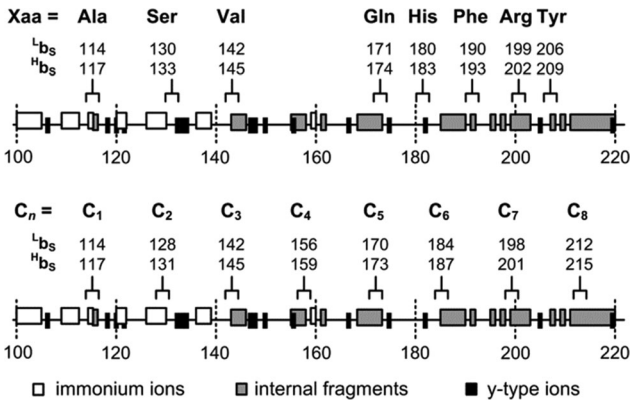

FIGURE 2. 2-Plex signal mass windows for Xaa- and C_n-tags. The *m/z* 100–220 range is ion-rich due to immonium ions, internal fragments, and y-type ions that can interfere with $^{L/H}\mathbf{b}_S$ signals. Ala-, Ser- and His-tags produce $^{L/H}\mathbf{b}_S$ signals in a quiet region, whereas Val-, Gln-, Phe-, Arg-, and Tyr-tags provide $^{L/H}\mathbf{b}_S$ signals in a pseudo-quiet region. The C_n-tags ($n = 1$–8) result in $^{L/H}\mathbf{b}_S$ signals sequentially with a 14-Da gap in a pseudo-quiet region. The C_n'-tags yield $^{L/H}\mathbf{b}_S$ signals at the same positions as the C_n-tags.

signal-variable MBITs allow the multiplexed quantification of peptides and proteins, enabling the $(N + 1)$-plex quantitation using *N* different sets of 2-plex MBITs (Suh et al., 2011). Furthermore, the $\mathbf{b}_S$ ion (N-protonated oxazolone) enables a precise measurement of ion temperature from the reaction yield of its subsequent unimolecular dissociation to the $\mathbf{a}_S$ ion (Seo et al., 2012), because the dissociation rate depends on the internal energy of the $\mathbf{b}_S$ ion which varies with the temperature of the peptide ion. Most importantly, the isotope-coded high-mass $^{H/L}\mathbf{y}_S$ ions (protonated Ala-peptides), unlike their complementary low-mass $^{L/H}\mathbf{b}_S$ ions, afford the isobaric quantification of peptides in the quadrupole ion trap (QIT) where a 1/3 mass cutoff problem hinders the use of other isobaric tags based on low-mass signals (Seo, Yoon, & Shin, 2011).

III. LOW-MASS QUANTITATION SIGNAL

Using matrix-assisted laser desorption/ionization (MALDI)-time-of-flight (TOF)/TOF and electrospray ionization (ESI)-quadrupole TOF (Q-TOF) mass spectrometers, low-mass quantitation signals have been examined by conjugating aliphatic C_n-tags to the model peptide bradykinin (RPPGFSPFR) (Suh et al., 2011). MALDI-MS yielded singly protonated MBIT-linked bradykinin (MH^+), whereas ESI-MS provided doubly protonated MBIT-linked bradykinin (MH_2^{2+}). The tandem mass spectra of MH^+ and MH_2^{2+} presented $^{L/H}\mathbf{b}_S$ ions as well as various sequence ions (Fig. 3). The positions of y-type ions having no MBIT at the *N*-terminus were unchanged, whereas those of a- and b-type ions containing MBIT were shifted by the mass difference of C_n amino acids. Both MH^+ and MH_2^{2+} generated $^{L/H}\mathbf{b}_S$ ions as the primary quantitation signals. Then, $^{L/H}\mathbf{b}_S$ ions underwent subsequent fragmentations, producing the secondary quantitation signals, $^{L/H}\mathbf{a}_S$ ions, after a loss of CO. The relative abundances of $^{L/H}\mathbf{b}_S$ and $^{L/H}\mathbf{a}_S$ ions showed that $^{L/H}\mathbf{a}_S$ signals from both MALDI-produced MH^+ and ESI-generated MH_2^{2+} gradually increased from C_1 to C_8 as the alkyl chain length increased, whereas $^{L/H}\mathbf{b}_S$ signals increased from C_1 to C_4 for MH^+ or C_6 for MH_2^{2+} and then decreased (Fig. 4).

A good linearity of quantitation was obtained for all aliphatic C_n-tags in the 15–250 fmol range when MBIT-linked peptides were analyzed in MALDI-MS/MS by varying the 2-plex mixing ratios from 1:1 to 1:16. The slopes of both $^L\mathbf{b}_S/^H\mathbf{b}_S$ and $^L\mathbf{a}_S/^H\mathbf{a}_S$ were close to 1 in the linearity plot of measured ratios versus premixed ratios. In comparison, a linearity up to 1:16–25 dilutions has been reported for other isobaric tags providing low-mass quantitation signals (Casado-Vela et al., 2010).

The LC elution profiles of the 1:1 2-plex MBIT-linked bradykinin were obtained by recording the intensities of $^{L/H}\mathbf{b}_S$ ions every 3 sec in the multiple-reaction monitoring (MRM) mode using LC-ESI-triple quadrupole/linear ion trap (Fig. 5). For C_1–C_8 tags, the isotopomeric peptides differentially labeled with each tag co-eluted in LC and their retention time increased stepwise as the length of alkyl chain increased, separating C_n-tagged bradykinin approximately 1–3 min apart. On average, the measured $^H\mathbf{b}_S/^L\mathbf{b}_S$ ratio was approximately 1.0 with a 10–12% fluctuation over the entire elution time for all aliphatic C_n-tags.

In the cases of Xaa-tags (our unpublished data), basic His- and Arg-tags had a tendency to increase the ionization efficiency in MALDI-MS and the charge state in ESI-MS.

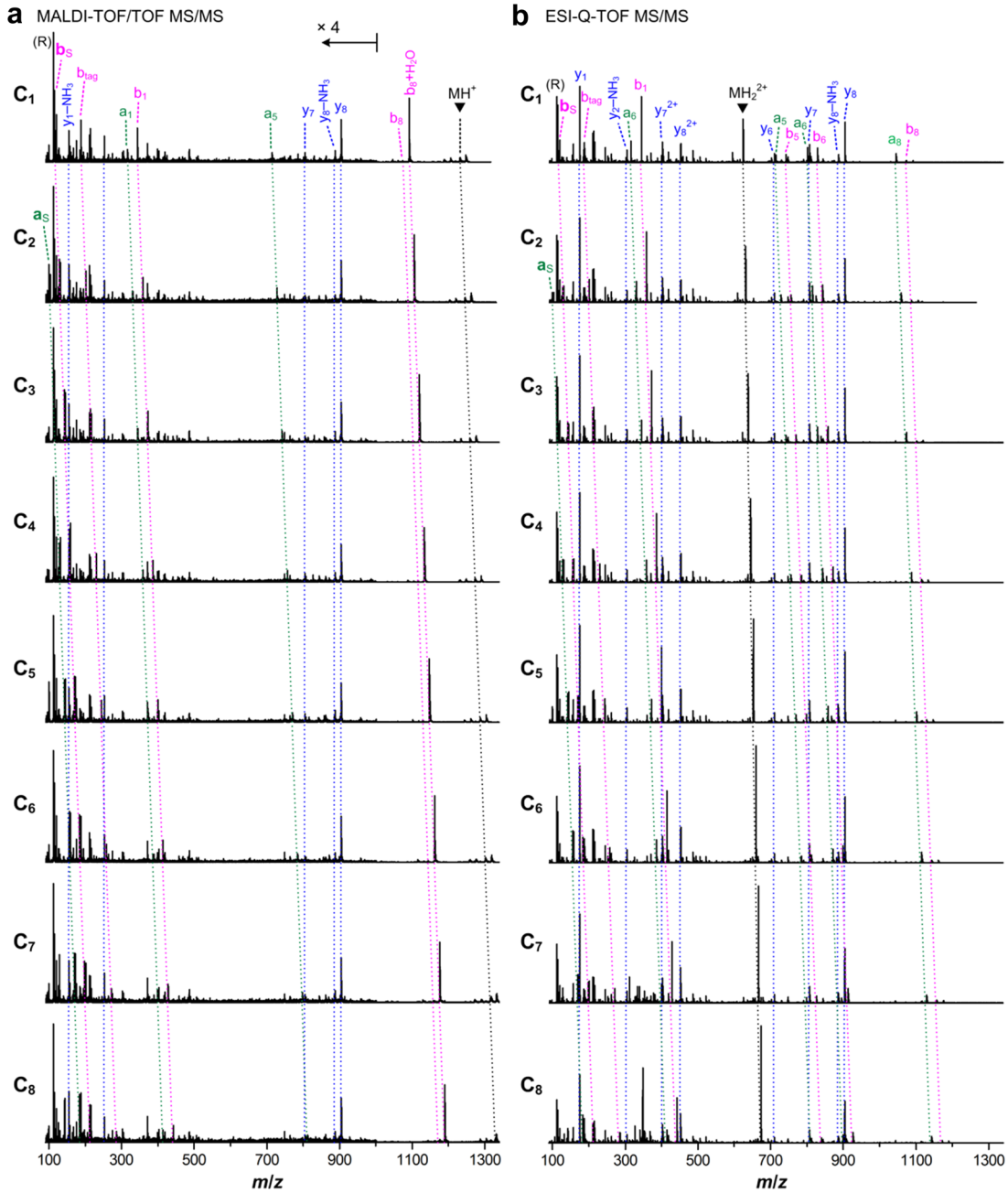

FIGURE 3. Tandem mass spectra of C_n-tagged bradykinin (*N*-Ac-C_nA-RPPGFSPFR, $n = 1$–8). (**a**) MALDI-MS/MS spectra of singly protonated C_n-tagged bradykinin (MH^+) obtained using TOF/TOF (Applied Biosystems 4700 Proteomics Analyzer, Foster City, CA) and (**b**) ESI-MS/MS spectra of doubly protonated C_n-tagged bradykinin (MH_2^{2+}) obtained using Q-TOF (Waters Q-TOF Premiere, Manchester, UK). The a-, b-, and y-type ions are colored in green, magenta, and blue, respectively. Both $\mathbf{a}_S$ and $\mathbf{b}_S$ ions are shown in bold. The precursor ions, MH^+ and MH_2^{2+}, are marked by inverted triangle.

While both His- and Gln-tags provided strong $^{L/H}\mathbf{b}_S$ signals, Ala- and Ser-tags presented relatively weak $^{L/H}\mathbf{b}_S$ signals. Also, the Gln-tag underwent the least secondary fragmentation producing the $^{L/H}\mathbf{a}_S$ ions. The Arg-tag uniquely generated $^{L/H}\mathbf{b}_S$–NH_3 ions as secondary quantitation signals. All Xaa-tags except for the Ser-tag exhibited a good linearity of quantitation in the 15–250 fmol range. The Ser-tag significantly underestimated the premixed ratio due to the overlap of $^{H}\mathbf{b}_S$ with an unidentified peak.

In brief, low-mass quantitation signals of MBITs are mass-tunable and enable the peptide quantification in the 15–250 fmol range.

IV. HIGH-MASS QUANTITATION SIGNAL

Low-mass quantitation signals are inaccessible to most QIT instruments because of the low mass cutoff in ion trapping during resonant excitation of the precursor ion (Payne &

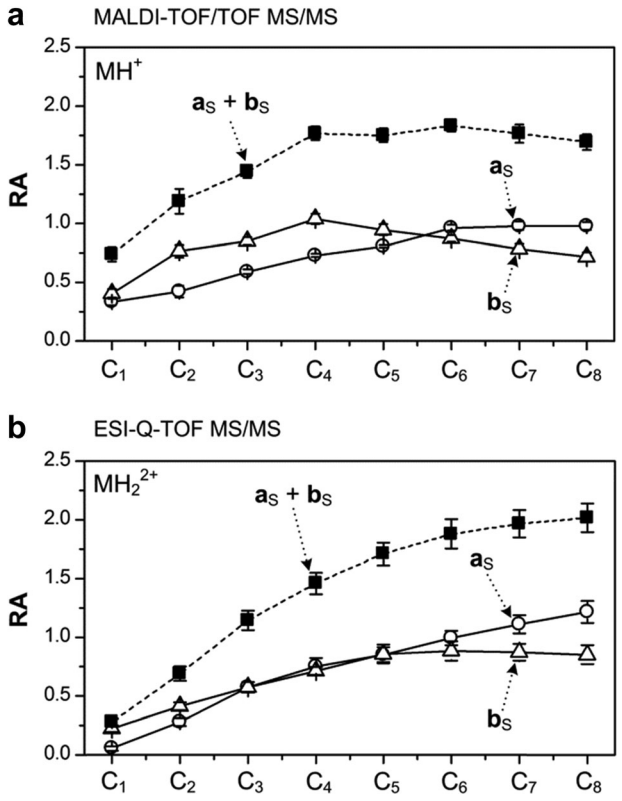

FIGURE 4. Relative abundances of low-mass quantitation signals, $\mathbf{a}_S$ (open circle) and $\mathbf{b}_S$ (open triangle), obtained from singly protonated C_n-tagged bradykinin (MH^+) (**a**) and doubly protonated C_n-tagged bradykinin (MH_2^{2+}) (**b**). Relative abundance is shown with respect to the arginine immonium ion at *m/z* 112. An error bar represents the standard deviation of six measurements. RA, relative abundance.

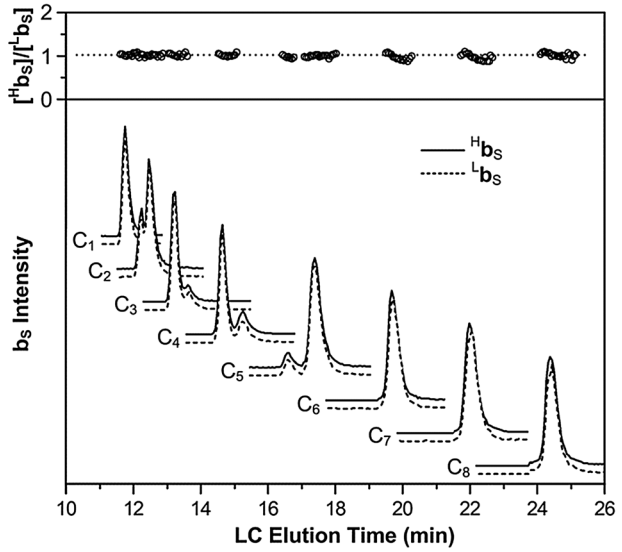

FIGURE 5. $^{H/L}\mathbf{b}_S$ ion chromatograms obtained from the 1:1 mixture of 2-plex C_n-tagged bradykinin using MRM mode in ESI-Q-TRAP MS/MS. Normalized intensities of $^{H}\mathbf{b}_S$ (solid line) and $^{L}\mathbf{b}_S$ ions (dotted line) derived from the doubly protonated precursor ions are displayed (bottom). Measured values of $[^{H}\mathbf{b}_S]/[^{L}\mathbf{b}_S]$ are plotted against LC elution time (top).

Glish, 2001; Griffin et al., 2007; Yang et al., 2009). Although this mass cutoff problem has been addressed recently by several groups (Cunningham, Glish, & Burinsky, 2006), it is still a significant drawback of conventional QIT mass spectrometers. In addition, the *m/z* 100–220 region is ion-rich due to other fragment peaks overlapping with the signal ions. MBITs can circumvent these problems by providing high-mass signals in a noise-free region for the accurate protein quantification (Seo, Yoon, & Shin, 2011).

To examine high-mass quantitation signals for peptide quantification, we conjugated the Gln-tag (Ac-QA-OSu) to two model peptides, LISFYAGR (**1**) and LISFYAGK (**2**), which have the same sequence except for the *C*-terminal amino acid (Seo, Yoon, & Shin, 2011). The amine-reactive coupling via the OSu-linker resulted in Ac-QA-LISFYAGR ($\mathbf{1}^1$) with one Gln-tag conjugated at the *N*-terminus and Ac-QA-LISFYAGK-AQ-Ac ($\mathbf{2}^2$) with two Gln-tags conjugated at the *N*-terminus and lysine. The numbers in superscript denote the number of tags attached to the peptides. The 1:1 mixture of 2-plex MBIT-linked peptides was prepared for both $\mathbf{1}^1$ and $\mathbf{2}^2$ and analyzed by using a QIT mass spectrometer equipped with an ESI source. The ESI mass spectra of $\mathbf{1}^1$ and $\mathbf{2}^2$ presented isotopomeric peaks of $[\mathbf{1}^1+\mathrm{H}]^+$, $[\mathbf{1}^1+2\mathrm{H}]^{2+}$, $[\mathbf{2}^2+\mathrm{H}]^+$, and $[\mathbf{2}^2+2\mathrm{H}]^{2+}$. The ESI-QIT MS/MS spectra showed $^{H/L}\mathbf{y}_S$ and $^{H/L}\mathbf{y}_S{}^{2+}$ ions. $^{H/L}\mathbf{y}_S$ ions were produced from singly protonated peptides after a loss of Ac-Q and also from doubly protonated peptides after a loss of the b_S ion ($[\text{Ac-Q}+\mathrm{H}]^+$). $^{H/L}\mathbf{y}_S{}^{2+}$ ions were derived from $[\mathbf{2}^2+2\mathrm{H}]^{2+}$ after a loss of Ac-Q. In the case of the arginine-terminated peptide $\mathbf{1}^1$, the relative abundance of $(^{H}\mathbf{y}_S+{}^{L}\mathbf{y}_S)$ was approximately 2% of the total fragment ions and the $[^{H}\mathbf{y}_S]/[^{L}\mathbf{y}_S]$ ratios of 1.05 and 1.02 were obtained for $[\mathbf{1}^1+\mathrm{H}]^+$ and $[\mathbf{1}^1+2\mathrm{H}]^{2+}$, respectively. For the lysine-terminated peptide $\mathbf{2}^2$, the relative abundances of $(^{H}\mathbf{y}_S+{}^{L}\mathbf{y}_S)$ were 48% for $[\mathbf{2}^2+\mathrm{H}]^+$ and 18% for $[\mathbf{2}^2+2\mathrm{H}]^{2+}$, and the $[^{H}\mathbf{y}_S]/[^{L}\mathbf{y}_S]$ ratio was 1.00 for both ions.

The quantitation linearity of the $^{H/L}\mathbf{y}_S$ signals was checked by mixing 2-plex MBIT-linked peptides $\mathbf{2}^2$ in various ratios. A linear relationship between measured and premixed $[^{H}\mathbf{y}_S]/[^{L}\mathbf{y}_S]$ ratios was observed for $[\mathbf{2}+2\mathrm{H}]^{2+}$ to the lowest amount of 270 fmol after 1:36 dilution. For $[\mathbf{2}+\mathrm{H}]^+$, a linearity was maintained to 150 fmol even after 1:64 dilution. Thus, the $^{H/L}\mathbf{y}_S$ signals enable the relative quantification of peptides showing a 36- to 64-fold difference in concentration. As mentioned before, low-mass signals derived from other isobaric tags show quantitation linearity until 1:16–25 dilutions.

The LC elution profiles of 2-plex MBIT-linked peptides $\mathbf{1}^1$ and $\mathbf{2}^2$ were also obtained by monitoring low-mass $^{L/H}\mathbf{b}_S$ ions for $[\mathbf{1}^1+\mathrm{H}]^+$ and high-mass $^{H/L}\mathbf{y}_S$ ions for $[\mathbf{2}^2+\mathrm{H}]^+$ through MRM using a triple quadrupole mass spectrometer connected to a nano-LC system (Fig. 6). In both cases, the 2-plexed peptides co-eluted and the measured L/H (or H/L) ratio was almost identical to the premixed ratio of 1.0. The $[^{L}\mathbf{b}_S]/[^{H}\mathbf{b}_S]$ ratio was 1.02 ± 0.07 and the $[^{H}\mathbf{y}_S]/[^{L}\mathbf{y}_S]$ ratio was 0.99 ± 0.05. Surely, both low-mass and high-mass quantitation signals faithfully reproduce the 1:1 premixed ratio of 2-plex MBIT-linked peptides. And the isobaric ^{1}H/^{2}H-labeling of *N*-acetyl dipeptide MBIT results in no ^{1}H/^{2}H-isotope effects (Zhang et al., 2001; Zhang & Regnier, 2002; Hansen et al., 2003; Yi et al., 2005) on the LC retention time of 2-plex MBIT-linked peptides.

Lastly, the performance of MBITs on protein quantification was demonstrated with a protein mixture containing horse

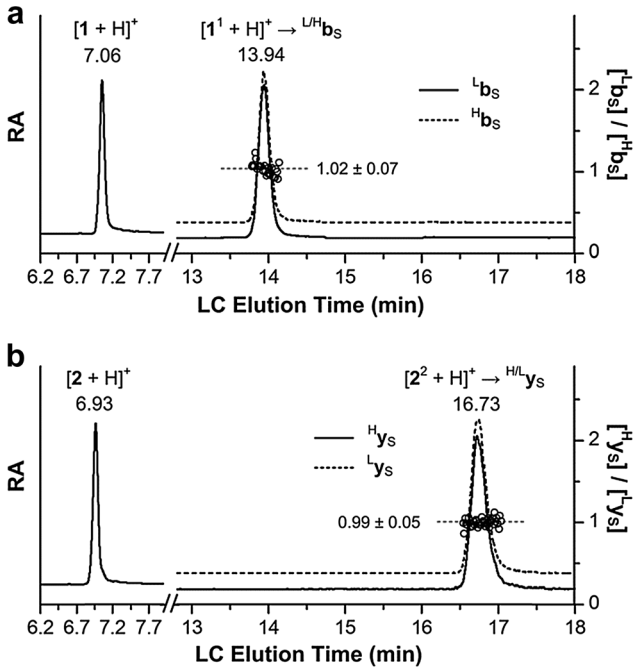

FIGURE 6. Extracted ion chromatograms of unmodified peptide **1** and $^{L/H}\mathbf{b}_S$ ions derived from one Gln-tagged peptide $\mathbf{1}^1$ (**a**), and unmodified peptide **2** and $^{H/L}\mathbf{y}_S$ ions derived from two Gln-tagged peptide $\mathbf{2}^2$ (**b**). ESI-MS and MS/MS spectra were obtained for unmodified peptides and product ions ($^{L/H}\mathbf{b}_S$ and $^{H/L}\mathbf{y}_S$), respectively, using a triple quadrupole mass spectrometer. RA, relative abundance.

myoglobin, bovine serum albumin (BSA), and human ubiquitin by using a linear QIT mass spectrometer connected to a nano-LC system (Seo, Yoon, & Shin, 2011). These proteins were mixed in two different ratios (samples A and B) and digested with trypsin. Tryptic peptides in samples A and B were

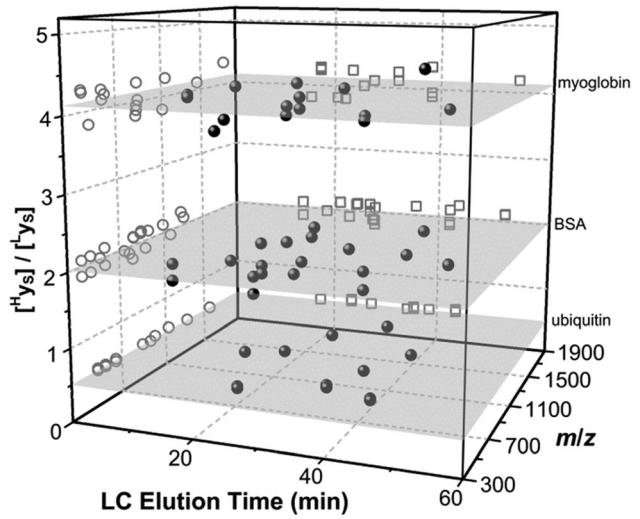

FIGURE 7. $[^H\mathbf{y}_S]/[^L\mathbf{y}_S]$ ratios as a function of LC elution time and *m/z* of Gln-tagged peptides. For LC-ESI-QIT MS/MS analyses, 2-plex Gln-tagged peptides were prepared from the two protein mixtures that contain different amounts of horse myoglobin, bovine serum albumin (BSA), and human ubiquitin. Open circle shows the $[^H\mathbf{y}_S]/[^L\mathbf{y}_S]$ ratio as a function of *m/z*, while open square exhibits the $[^H\mathbf{y}_S]/[^L\mathbf{y}_S]$ ratio as a function of LC elution time. Each shaded plane represents the average of all $[^H\mathbf{y}_S]/[^L\mathbf{y}_S]$ ratios (solid sphere) obtained by elution time and *m/z* for each protein.

differentially labeled with 2-plex MBITs. Figure 7 shows the $[^H\mathbf{y}_S]/[^L\mathbf{y}_S]$ ratios as a function of LC elution time and *m/z*. Lysine-terminated peptides were present in the 1+ and 2+ charge states, whereas arginine-terminated peptides were in the 1+, 2+, and 3+ charge states. Mascot MS/MS ion search successfully identified 10, 15, and 7 MBIT-linked peptides from myoglobin, BSA, and ubiquitin, respectively. Singly charged (protonated) peptides yielded $^{H/L}\mathbf{y}_S$ ions, doubly charged peptides resulted in both $^{H/L}\mathbf{y}_S$ and $^{H/L}\mathbf{y}_S{}^{2+}$ ions, and triply charged peptides produced both $^{H/L}\mathbf{y}_S{}^{2+}$ and $^{H/L}\mathbf{y}_S{}^{3+}$ ions. Of the three charge-state ions, both $^{H/L}\mathbf{y}_S$ and $^{H/L}\mathbf{y}_S{}^{2+}$ ions were used for quantification. The measured $[\text{protein}]_A/[\text{protein}]_B$ ratios determined from $[^H\mathbf{y}_S]/[^L\mathbf{y}_S]$ values (4.13 ± 0.11 for myoglobin, 2.01 ± 0.06 for BSA, and 0.49 ± 0.02 for ubiquitin) were in excellent agreement with the premixed ratios (4.0 for myoglobin, 2.0 for BSA, and 0.5 for ubiquitin), showing an error within 4%. Thus, both lysine- and arginine-terminated, MBIT-linked peptides offer high-mass signals for the accurate protein quantification.

V. MULTI 2-PLEX PROTEIN QUANTITATION

While the 2-plex MBIT-linked peptides co-migrate in LC, peptides labeled by different MBITs elute separately and show 2-plex quantitation signals in distinct mass windows. Thus, a combination of different MBITs enables the multi 2-plex quantification of proteins in a single LC-MS experiment. This multi 2-plex quantification strategy has been demonstrated by using Xaa-tags.

Xaa-tags were applied to the quantification of the yeast heat shock protein Hsp82p expressed under various chemical treatments. Hsp82p belongs to the mammalian Hsp90p family which serves as a molecular chaperone and regulates physiological roles of key proteins. Of the Xaa-tags, Phe-, Tyr-, Gln-, and His-tags were applied to the 5-plex quantification of Hsp82p expressed under the exposure to Hsp90p-specific inhibitor geldanamycin (10 μM and 20 μM), chromosome segregation inhibitor incentrom A (100 μM) (Yoon, 2004; Lee et al., 2008), anti-microtubule agent nocodazole (100 μM), and the solvent control, dimethyl sulfoxide (DMSO), to compare the effects of these small molecules on the expression level of Hsp82p. Each Hsp82p was purified by antibody-affinity, separated by sodium dodecyl sulfate–polyacrylamide gel electrophoresis, visualized by SYPRO Ruby staining, and then quantified by optical imaging and tandem mass spectrometry.

The optical imaging showed that the amount of Hsp82p on a gel was in the range of 2.2–5.2 μg and the ratios of inhibitor-treated to control Hsp82p levels were 1.00 for geldanamycin (10 μM), 1.08 for geldanamycin (20 μM), 0.46 for incentrom A (100 μM), and 0.60 for nocodazole (100 μM) (Fig. 8a). For the LC-MS/MS experiment, each Hsp82p was in-gel digested with trypsin and their tryptic peptides were separately labeled with the CD_3/CH_3-form of Phe-, Tyr-, Gln-, or His-tag (Fig. 8b). Meanwhile, tryptic peptides of the DMSO-treated sample (control) were divided into four aliquots and each aliquot was separately labeled with the CH_3/CD_3-form of each Xaa-tag. All of the MBIT-linked peptides were mixed together, separated by LC, and analyzed by MALDI-MS and -MS/MS. The 2-plex quantitation signals from each Xaa-tag resulted in the ratios of inhibitor-treated to DMSO-treated Hsp82p levels. The measured $[^H\mathbf{b}_S]/[^L\mathbf{b}_S]$ ratios are shown in Figure 8c as a function of LC

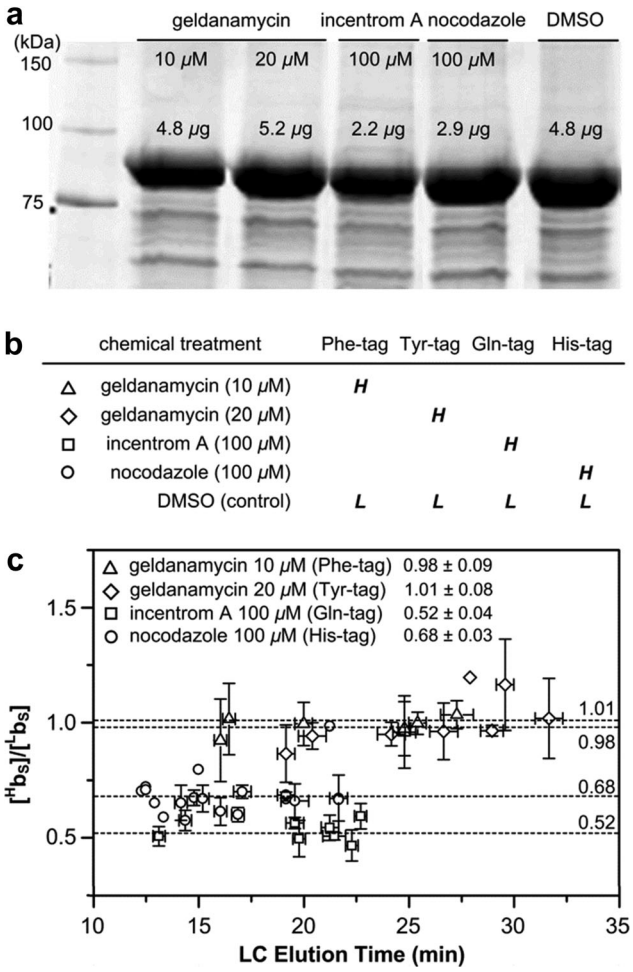

FIGURE 8. Multi 2-plex quantitation of the yeast Hsp82p levels expressed under different chemical stresses. (**a**) SYPRO Ruby-stained gel of Hsp82p isolated from the yeast proteome using anti-hemagglutinin affinity beads. Hsp82p was expressed in the presence of geldanamycin (10 μM), geldanamycin (20 μM), incentrom A (100 μM), nocodazole (100 μM), and DMSO alone. All four chemicals were dissolved in DMSO. (**b**) Tagging scheme for 5-plex quantification of Hsp82p. The chemical-treated samples were separately labeled with the CD_3/CH_3-forms (*H*) of four different Xaa-tags (Phe-, Tyr-, Gln-, and His-tags). The DMSO-treated sample (control) was labeled with the CH_3/CD_3-forms (*L*) of four Xaa-tags. All eight MBIT-linked samples were mixed together and analyzed by LC-MALDI-TOF/TOF MS/MS. (**c**) $[^{H}\mathbf{b}_S]/[^{L}\mathbf{b}_S]$ ratios plotted against LC elution time. Error bars along the *x*- and *y*-axis refer to the spread in elution time and the standard deviation of average *H*/*L* ratio, respectively.

elution time. MBIT-linked peptides eluted in the order of His-, Gln-, Tyr-, and Phe-tags. The average ratios of inhibitor-treated to DMSO-treated Hsp82p levels were 0.98 ± 0.09 for geldanamycin (10 μM), 1.01 ± 0.08 for geldanamycin (20 μM), 0.52 ± 0.04 for incentrom A (100 μM), and 0.68 ± 0.03 for nocodazole (100 μM). These ratios obtained from 40 to 90 ng of peptides using MBITs are in accord with those obtained from 2 to 5 μg of peptides using optical imaging within a 2–12% error.

Of the aliphatic C_n-tags, C_6–C_8 tags have been successfully applied to the 4-plex quantification of the yeast Hsc82p (an isoform of Hsp82p) expressed in the presence or absence of Hsp82p to see if a loss of Hsp82p affects the amounts of Hsc82p under the heat-shock condition (Suh et al., 2011).

These results demonstrate the capability of signal-variable MBITs for the multi 2-plex quantification of proteins at the nanogram level. It is noteworthy that our multiplexing strategy requires more reactions than other multiplex isobaric reagents. Nonetheless, signal-variable MBITs can serve as a versatile tool for the MS-based quantitative proteomics.

VI. MEASUREMENT OF ION TEMPERATURE USING N-PROTONATED OXAZOLONE

The b-type ion (N-protonated oxazolone) undergoes a unimolecular dissociation through the transition state involving cleavage of both O(1)—C(5) and C(4)—C(5) bonds, releasing C(5)O(6), and the resulting a-type ion has the structure of protonated imine (Paizs et al., 2000; El Aribi et al., 2003; Harrison et al., 2004) (Fig. 9). The MS/MS spectra of MBIT-linked peptides show both $\mathbf{a}_S$ and $\mathbf{b}_S$ ions as low-mass quantitation signals. Since the $\mathbf{b}_S$ ion dissociates to the $\mathbf{a}_S$ ion, the $\mathbf{a}_S$-ion yield obtained from this unimolecular CO-loss process can be used to measure the temperature of the $\mathbf{b}_S$ ion (Seo et al., 2012).

The CH_3/CD_3-forms of both C_n- and C_n'-tags ($n = 1$–8) were conjugated to the *N*-termini of sample peptide, [Glu^1]-fibrinopeptide B. Singly and doubly protonated peptide ions labeled with C_n- or C_n'-tags were produced by MALDI and ESI, respectively. CID of the tagged peptide ions produced the $\mathbf{b}_S$ ion from the tag: N-protonated 2-methyl-4-alkyloxazol-5-one ($\mathbf{b}_S$) from the C_n-tag and N-protonated 2-alkyl-4-methyloxazol-5-one ($\mathbf{b}_S'$) from the C_n'-tag. Yields of $\mathbf{a}_S$ or $\mathbf{a}_S'$ ions derived from $\mathbf{b}_S$ or $\mathbf{b}_S'$ ions varied with the chain length and position of the alkyl substituent on N-protonated oxazolone. As the length of alkyl side chain on the C_n- or C_n'-tag was extended from C_1 to C_8, the yield of the $\mathbf{a}_S$ ion gradually increased for 4-alkyl-substituted oxazolone ($\mathbf{b}_S$) and decreased for 2-alkyl-substituted one ($\mathbf{b}_S'$) (Fig. 10). According to the potential energy surface obtained from ab initio calculations, the 4-alkyl substitution of *N*-protonated oxazolone decreases the enthalpy of activation ($\Delta H^{\ddagger}$) by stabilizing the transition state, whereas the 2-alkyl substitution increases $\Delta H^{\ddagger}$ by stabilizing the reactant. Both microcanonical and canonical rate constants were calculated for the CO-loss process, and activation energies and pre-exponential factors for this reaction were obtained from Arrhenius plots of canonical rate constants. These activation parameters were then used to calculate the $\mathbf{a}_S$-ion yield as a function of temperature by considering the transit time of the $\mathbf{b}_S$ ion in a collision cell. The comparison of theroretical $\mathbf{a}_S$-ion yields with experimental ones

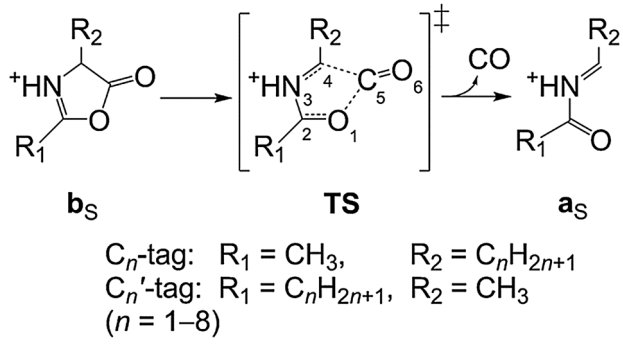

FIGURE 9. Unimolecular dissociation of N-protonated oxazolone ($\mathbf{b}_S$) to protonated imine ($\mathbf{a}_S$) and CO via transition state (**TS**).

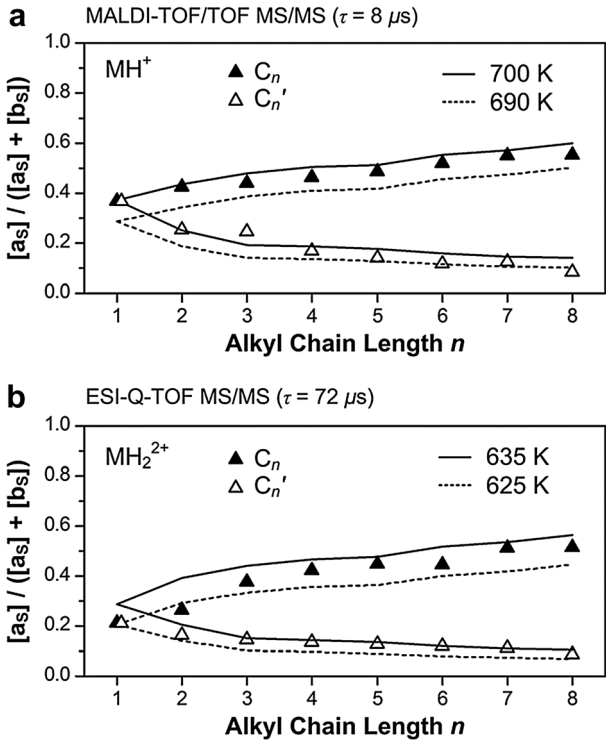

FIGURE 10. Yield of the $\mathbf{a}_S$ ion, $[\mathbf{a}_S]/[\mathbf{a}_S + \mathbf{b}_S]$, obtained from the MALDI-TOF/TOF MS/MS spectra (**a**) and the ESI-Q-TOF MS/MS spectra (**b**). [Glu^1]-fibrinopeptide B was labeled with the C_n-tag (solid triangle) and the C_n'-tag (open triangle). MALDI-MS yielded singly protonated peptide ions (MH^+) and ESI-MS provided doubly protonated peptide ions (MH_2^{2+}). Both singly and doubly protonated peptide ions resulted in singly charged $\mathbf{a}_S$ and $\mathbf{b}_S$ ions. Theoretical $\mathbf{a}_S$-ion yields calculated at the two different temperatures are presented as solid and dotted lines. Although the $\mathbf{a}_S$-ion yield significantly varies with the tag and alkyl chain length, the $\mathbf{b}_S$-ion temperature is nearly identical: 695 ± 5 K in MALDI-TOF/TOF MS/MS ($\tau = 8$ μs) and 630 ± 5 K in ESI-Q-TOF MS/MS ($\tau = 72$ μs). τ is the transit time of the peptide ion in a collision cell.

allowed a precise determination of the $\mathbf{b}_S$-ion temperature (Fig. 10). The $\mathbf{a}_S$-ion yield was a measure of ion temperature from the tandem mass spectra. Remarkably, the $\mathbf{b}_S$-ion temperatures from both C_n- and C_n'-tags ($n = 1$–8) were nearly the same with a few degree difference. Moreover, when the $\mathbf{b}_S$-ion temperatures were nearly identical, the y-type fragment patterns were similar, even though the b-type fragment patterns varied with the tag and alkyl chain length. Thus, MBITs can be used as internal temperature standards that enable a reproducible acquisition of the peptide tandem mass spectra.

VII. CONCLUDING REMARKS

Isobaric mass tags have been widely used as a robust tool for the MS-based quantitative analysis of proteins in life sciences. Accurate quantification and identification of whole proteins provide global as well as specialized landscape of the proteome at physiological states. By detecting specific changes in the proteome homeostasis, quantitative proteomics can provide insight into the cellular roles of individual proteins under normal conditions and result in the identification of biomarkers defining pathological states. The discovery of such biomarkers requires low-cost, sensitive, and multiplexed isobaric tags that can be generally applied to diverse MS-platforms. Also, it is necessary to increase the quantitation accuracy by enhancing the separation efficiency of precursor peptides for the LC-MS/MS analysis. MBITs can tackle some of these problems by employing low-cost $^1H/^2H$ isotopes, by offering high-mass quantitation signals, and by varying low-mass signal windows and elution properties of multiple tag-conjugated peptides. However, MBIT lacks the ability to enrich tag-conjugated peptides. A cleavable affinity moiety could be incorporated into MBITs to improve the performance of MBITs in quantitative proteomics. This should greatly reduce the sample size and also facilitate the detection of low-level peptides.

One of the major challenges in the peptide (or biomolecule) mass spectrometry has been the standardization of the mass spectral data to build a library. Since the peptide fragmentation is typically induced by collision after ionization (MALDI or ESI), the temperature of the collisionally activated peptide ion can serve as an internal standard. MBITs can be used to measure the ion temperature in the course of tandem mass spectrometry and assign a temperature to the peptide mass spectra, similarly to the thermal (black-body) radiation curves. A collection of temperature-assigned peptide mass spectra should help compiling a standard library for the peptide mass spectrometry. Thus, MBITs can be used in the peptide tandem mass spectrometry to provide the temperature-assigned mass spectra of peptides as well as quantitative information in all types of platforms for MS-based proteomics.

VIII. ABBREVIATIONS

BSA	bovine serum albumin
CILAT	cysteine-specific cleavable isobaric-labeled affinity tag
CID	collision-induced dissociation
CIT	Caltech isobaric tag
DiART	deuterium isobaric amine-reactive tag
DiLeu	N,N-dimethylated leucine tag
DMSO	dimethyl sulfoxide
ESI	electrospray ionization
iTRAQ	isobaric tags for relative and absolute quantitation
LC	liquid chromatography
MALDI	matrix-assisted laser desorption/ionization
MBIT	mass-balanced $^1H/^2H$-isotope-coded dipeptide tag
MRM	multiple reaction monitoring
MS	mass spectrometry
MS/MS	tandem mass spectrometry
OSu	*N*-succinimidyl ester
QIT	quadrupole ion trap
Q-TOF	quadrupole time-of-flight
TMT	tandem mass tag
TOF	time-of-flight

ACKNOWLEDGMENTS

J.S. acknowledges the postdoctoral support from the Brain Korea 21 program administered by the Ministry of Education, Science and Technology (MEST) of Korea. This work was supported by the Functional Proteomics Center grant (no.

FPR08A1-040) and the National Research Foundation grant (no. 2009-0086218) funded by MEST.

REFERENCES

Aebersold R, Mann M. 2003. Mass spectrometry-based proteomics. Nature 422:198–207.

Biemann K, Martin SA. 1987. Mass spectrometric determination of the amino acid sequence of peptides and proteins. Mass Spectrom Rev 6:1–75.

Casado-Vela J, Martínez-Esteso MJ, Rodriguez E, Borrás E, Elortza F, Bru-Martínez R. 2010. iTRAQ-based quantitative analysis of protein mixtures with large fold change and dynamic range. Proteomics 10:343–347.

Choe L, D'Ascenzo M, Relkin NR, Pappin D, Ross P, Williamson B, Guertin S, Pribil P, Lee KH. 2007. 8-plex quantitation of changes in cerebrospinal fluid protein expression in subjects undergoing intravenous immunoglobulin treatment for Alzheimer's disease. Proteomics 7:3651–3660.

Cunningham C, Glish GL, Burinsky DJ. 2006. High amplitude short time excitation: A method to form and detect low mass product ions in a quadrupole ion trap mass spectrometer. J Am Soc Mass Spectrom 17:81–84.

Dayon L, Hainard A, Licker V, Turck N, Kuhn K, Hochstrasser DF, Burkhard PR, Sanchez JC. 2008. Relative quantification of proteins in human cerebrospinal fluids by MS/MS using 6-plex isobaric tags. Anal Chem 80:2921–2931.

Dayon L, Turck N, Kienle S, Schulz-Kanppe P, Hochstrasser DF, Scherl A, Sanchez JC. 2010. Isobaric tagging-based selection and quantitation of cerebrospinal fluid tryptic peptides with reporter calibration curves. Anal Chem 82:848–858.

Dongré AR, Jones JL, Somogyi Á, Wysocki VH. 1996. Influence of peptide composition, gas-phase basicity, and chemical modification on fragmentation efficiency: Evidence for the mobile proton model. J Am Chem Soc 118:8365–8374.

El Aribi H, Rodriquez CF, Almeida DR, Ling Y, Mak WW, Hopkinson AC, Siu KWM. 2003. Elucidation of fragmentation mechanisms of protonated peptide ions and their products: A case study on glycylglycylglycine using density functional theory and threshold collision-induced dissociation. J Am Chem Soc 125:9229–9236.

Eng JK, McCormack AL, Yates JR. 1994. An approach to correlate tandem mass spectral data of peptides with amino acid sequences in a protein database. J Am Soc Mass Spectrom 5:976–989.

Griffin TJ, Xie H, Bandhakavi S, Popko J, Mohan A, Carlis JV, Higgins L. 2007. iTRAQ reagent-based quantitative proteomic analysis on a linear ion trap mass spectrometer. J Proteome Res 8:4665–4675.

Gygi SP, Rist B, Gerber SA, Turecek F, Gelb MH, Aebersold R. 1999. Quantitative analysis of complex protein mixtures using isotope-coded affinity tags. Nat Biotechnol 17:994–999.

Hansen KC, Schmitt-Ulms G, Chalkley RJ, Hirsch J, Baldwin MA, Burlingame AL. 2003. Mass spectrometric analysis of protein mixtures at low levels using cleavable ^{13}C-isotope-coded affinity tag and multidimensional chromatography. Mol Cell Proteomics 2:299–314.

Harrison AG, Young AB, Schnoelzer M, Paizs B. 2004. Formation of iminium ions by fragmentation of a_2 ions. Rapid Commun Mass Spectrom 18:1635–1640.

Lee HY, Jung Y, Kim W, Kim JH, Suh MS, Shin SK, Yoon HJ. 2008. Structure-activity relationship studies of the chromosome segregation inhibitor, Incentrom A. Bioorg Med Chem Lett 18:4670–4674.

Li S, Zeng D. 2007. CILAT—A new reagent for quantitative proteomics. Chem Commun 2181–2183.

McAlister GC, Huttlin EL, Haas W, Ting L, Jedrychowski MP, Rogers JC, Kuhn K, Pike I, Grothe RA, Blethrow JD, Gygi SP. 2012. Increasing the multiplexing capacity of TMTs using reporter ion isotopologues with isobaric masses. Anal Chem 84:7469–7478.

Nold MJ, Wesdemiotis C, Yalcin T, Harrison AG. 1997. Amide bond dissociation in protonated peptides. Structures of the N-terminal ionic and neutral fragments. Int J Mass Spectrom Ion Processes 164:137–153.

Ong SE, Mann M. 2005. Mass spectrometry-based proteomics turns quantitative. Nat Chem Biol 1:252–262.

Paizs B, Lendvay G, Vékey K, Suhai S. 1999. Formation of b_2^+ ions from protonated peptides: An ab initio study. Rapid Commun Mass Spectrom 13:525–533.

Paizs B, Suhai S. 2005. Fragmentation pathways of protonated peptides. Mass Spectrom Rev 24:508–548.

Paizs B, Szlávik Z, Lendvay G, Vékey K, Suhai S. 2000. Formation of a_2^+ ions of protonated peptides. An ab initio study. Rapid Commun Mass Spectrom 14:746–755.

Payne AH, Glish GL. 2001. Thermally assisted infrared multiphoton photodissociation in a quadrupole ion trap. Anal Chem 73:3542–3548.

Polfer NC, Oomens J, Suhai S, Paizs B. 2005. Spectroscopic and theoretical evidence for oxazolone ring formation in collision-induced dissociation of peptides. J Am Chem Soc 127:17154–17155.

Rodríguez-Suárez E, Whetton AD. 2013. The application of quantification techniques in proteomics for biomedical research. Mass Spectrom Rev 32:1–26.

Roepstorff P, Fohlman J. 1984. Proposal for a common nomenclature for sequence ions in mass spectra of peptides. Biomed Mass Spectrom 11:601.

Ross PL, Huang YN, Marchese JN, Williamson B, Parker K, Hattan S, Khainovski N, Pillai S, Dey S, Daniels S, Purkayastha S, Juhasz P, Martin S, Barlet-Jones M, He F, Jacobson A, Pappin DJ. 2004. Multiplexed protein quantitation in *Saccharomyces cerevisiae* using amine-reactive isobaric tagging reagents. Mol Cell Proteomics 3:1154–1169.

Seo J, Suh MS, Thangadurai TD, Kim J, Rhee YH, Yoon HJ, Shin SK. 2008. Mass-balanced ^{1}H/^{2}H isotope dipeptide tag for simultaneous protein quantitation and identification. Anal Chem 80:6145–6153.

Seo J, Suh MS, Yoon HJ, Shin SK. 2012. *N*-acylated dipeptide tags enable precise measurement of ion temperature in peptide fragmentation. J Phys Chem B 116:13982–13990.

Seo J, Yoon HJ, Shin SK. 2011. Quantification of tryptic peptides in quadrupole ion trap using high-mass signals derived from isotope-coded *N*-acetyl dipeptide tags. J Am Soc Mass Spectrom 22:1668–1677.

Sohn CH, Lee JE, Sweredoski MJ, Graham RLJ, Smith GT, Hess S, Czerwieniec G, Loo JA, Deshaies RL, Beauchamp JL. 2012. Click chemistry facilitates formation of reporter ions and simplified synthesis of amine-reactive multiplexed isobaric tags for protein quantification. J Am Chem Soc 134:2672–2680.

Suh MS, Seo J, Thangadurai TD, Rhee YH, Shin SK, Yoon HJ. 2011. Aliphatic dipeptide tags for multi-2-plex protein quantification. Analyst 136:1614–1619.

Thompson A, Schäfer J, Kuhn K, Kienle S, Schwarz J, Schmidt G, Neumann T, Johnstone R, Mohammed AK, Hamon C. 2003. Tandem mass tags: A novel quantification strategy for comparative analysis of complex protein mixtures by MS/MS. Anal Chem 75:1895–1904.

Wenger CD, Lee MV, Hebert AS, McAlister GC, Phanstiel DH, Westphall MS, Coon JJ. 2011. Gas-phase purification enables accurate, multiplexed proteome quantification with isobaric tagging. Nat Methods 8:933–935.

Xiang F, Ye H, Chen R, Fu Q, Li L. 2010. *N*,*N*-dimethyl leucines as novel isobaric tandem mass tags for quantitative proteomics and peptidomics. Anal Chem 82:2817–2825.

Yang YH, Lee K, Jang KS, Kim YG, Park SH, Lee CS, Kim BG. 2009. Low mass cutoff evasion with q(z) value optimization in ion trap. Anal Biochem 387:133–135.

Yi EC, Li XJ, Cooke K, Lee H, Raught B, Page A, Aneliunas V, Hieter P, Goodlett DR, Aebersold R. 2005. Increased quantitative proteome coverage with ^{13}C/^{12}C-based acid-cleavable isotope-coded affinity

tag reagent and modified data acquisition scheme. Proteomics 5:380–387.

Yoon HJ. 2004. A novel small-molecule inhibitor of the chromosome segregation process in yeast. Mol Genet Genomics 271:490–498.

Yoon SH, Chamot-Rooke J, Perkins BR, Hilderbrand AE, Poutsma JC, Wysocki VH. 2008. IRMPD spectroscopy shows that AGG forms an oxazolone b_2^+ ion. J Am Chem Soc 130:17644–17645.

Zeng D, Li S. 2009a. Improved CILAT reagents for quantitative proteomics. Bioorg Med Chem Lett 19:2059–2061.

Zeng D, Li S. 2009b. Revival of deuterium-labeled reagents for protein quantitation. Chem Commun 3369–3371.

Zhang J, Wang Y, Li S. 2010. Deuterium isobaric amine-reactive tags for quantitative proteomics. Anal Chem 82:7588–7595.

Zhang R, Regnier FE. 2002. Minimizing resolution of isotopically coded peptides in comparative proteomics. J Proteome Res 1:139–147.

Zhang R, Sioma CS, Wang S, Regnier FE. 2001. Fractionation of isotopically labeled peptides in quantitative proteomics. Anal Chem 73:5142–5149.